

# Efficient Model Order Reduction Including Skin Effect

Shizhong Mei

Electrical and Computer Engineering  
Northwestern University  
Evanston, IL 60208  
1-847-467-7852

meisz@ece.northwestern.edu

Chirayu Amin

Electrical and Computer Engineering  
Northwestern University  
Evanston, IL 60208  
1-847-467-7852

c-amin@northwestern.edu

Yehea I. Ismail

Electrical and Computer Engineering  
Northwestern University  
Evanston, IL 60208  
1-847-467-7852

ismail@ece.northwestern.edu

## ABSTRACT

Skin effect makes interconnect resistance and inductance frequency dependent. This paper addresses the problem of efficiently estimating the signal characteristics of any *RLC* network when skin effect is significant, which complicates interconnect simulation. In this paper, a new type of moments is defined that simplifies the interconnect simulation, namely, the square root moments. The time to calculate the square root moments is similar to the time to calculate the traditional moments, and the new moments preserve the recursive properties of the traditional moments. Hence, the method introduced here can handle the more complex problem of interconnect simulation with skin effect at almost no overhead compared to constant element interconnect simulation. Using the square root moments, higher order approximations can be reached as compared to traditional moments. Also, the PVL method is modified to implicitly match the square root moments. The simulation results reveal the high accuracy of the proposed methods as well as the apparent variation in the signal characteristics caused by skin effect.

## Categories and Subject Descriptors

J.6 [Computer-Aided Engineering]: Computer-aided design (CAD), B.7.2 [Integrated Circuits]: Design Aids—Simulation.

## General Terms

Algorithms, Performance, Design, Theory.

## Keywords

Simulation, RLC, skin effect, model order reduction, VLSI

## 1. INTRODUCTION

In deep sub-micrometer technologies, the intrinsic gate delay tends to decrease dramatically. However, since the average length of global interconnect lines increases, interconnect delay

dominates the overall gate delay in current deep sub-micrometer VLSI circuits [1], [2]. To achieve high quality circuit design in as short a period of time as possible, it is necessary to accurately model interconnect lines and to find efficient algorithms for quick delay estimation and circuit simulation.

The increasing on-chip clock frequencies make skin effect on some nets, *e.g.*, clock and power distribution networks, increasingly prominent and non-negligible. Consequently, model order reduction techniques for constant element circuits (no frequency dependence) become inaccurate when skin effect is encountered. Existing work dealing with skin effect focuses on building models for SPICE or generates too complex models for quick delay estimation for an *RLC* network, *e.g.*, [3]-[5]. However, the standard tools for large VLSI circuits use model order reduction techniques. Hence, model order reduction techniques are required which can handle frequency dependent elements.

Many papers, *e.g.*, [6]-[8] have shown that the skin effect impedance can be described by  $A + B\sqrt{s}$  with high accuracy. Thus, this approximation is used in this paper. To deal with the square root term  $\sqrt{s}$ , a new type of moments is defined that simplifies the interconnect simulation, namely, the square root moments. Similar to the moments in case of constant elements, the square root moments obtained in this paper have the same recursive properties and are easy to calculate. Also, the PVL method is modified to include skin effect.

The rest of this paper is organized as follows. A background for skin impedance models and calculating delay in *RLC* circuits with constant elements is presented in section 2. The square root moments of general *RLC* trees and grids with skin effect are derived in section 3. The computation of time domain signals from the square root moments is given in section 4. The modified PVL method is explained in section 5. The simulated node voltages of several sample circuits are offered in section 6. Finally, some conclusions are given in section 7.

## 2. BACKGROUND

In the  $s$  domain, the transfer function of any constant *RLC* circuit takes the following general form

$$H(s) = \frac{1 + a_1s + a_2s^2 + \dots + a_{N-1}s^{N-1}}{b_0 + b_1s + b_2s^2 + \dots + b_Ns^N} \quad (1)$$

This research has been supported in part by National Science Foundation CAREER Award #CCR-0237822, Intel gifts and grants, and the Semiconductor Research Corporation (SRC).

Permission to make digital or hard copies of all or part of this work for personal or classroom use is granted without fee provided that copies are not made or distributed for profit or commercial advantage and that copies bear this notice and the full citation on the first page. To copy otherwise, or republish, to post on servers or to redistribute to lists, requires prior specific permission and/or a fee.

*DAC 2003*, June 2-6, 2003, Anaheim, California, USA.

Copyright 2003 ACM 1-58113-688-9/03/0006...\$5.00.

where  $a_i$ 's and  $b_i$ 's are real positive coefficients. The Taylor expansion of  $H(s)$  exists and is given by

$$H(s) = H^{(0)} + H^{(1)}s + \dots + \frac{H^{(k)}(0)}{k!}s^k + \dots \quad (2)$$

In order to efficiently evaluate the transient response, a popular method [9] is to match the leading moments of a reduced transfer function with the leading moments in the above expansion and use the reduced transfer function to obtain the inverse Laplace transform. Arbitrary accuracy can be achieved by matching higher number of additional moments. Elmore and Wyatt used only two terms of the expansion in (2) to find a closed form solution of the delay [10], [11]. The Wyatt approximation was extended in [12] to include the inductance of the interconnect. The capability of efficiently estimating the transient response makes the approximate methods mentioned above widely used in industry. Since the derived results do not apply to circuits with skin effect, it is desirable to find a new method that aims at calculating the transient response of circuits with skin effect with similar efficiency.

Skin effect impedance of conductors of arbitrary cross section can be accurately approximated by  $A + B\sqrt{s}$  [8]. The validity of this claim lies in the common behavior of impedance of any conductor. The impedance approaches the dc resistance at low frequency and is proportional to  $\sqrt{s}$  at high frequency. At intermediate frequencies, the frequency dependence of the impedance more or less matches the simple dc/ $\sqrt{s}$  skin effect model. A quantitative analysis of the impedance of round conductors will suffice to elaborate this explanation.

For conductors of circular cross section, its skin effect impedance can be expressed in a closed form [13] as

$$Z_i = -\frac{T}{2\pi r \sigma} \frac{J_0(Tr)}{J_0'(Tr)} \quad (3)$$

or equivalently as

$$Z_i = \frac{R_0}{2} j \sqrt{\frac{2s}{w_c}} \frac{J_0(-j\sqrt{\frac{2s}{w_c}})}{J_0'(-j\sqrt{\frac{2s}{w_c}})} \quad (4)$$

where  $R_0$  is the dc resistance and  $w_c$  is the frequency where the penetration depth equals the radius of the cross section of the conductor. Using the asymptotical expression of the Bessel function  $J_0(-j\sqrt{2s/w_c})$  in the limit  $s \rightarrow +j\infty$ , the following equality can be obtained

$$J_0'(-j\sqrt{\frac{2s}{w_c}})(0.5j\sqrt{\frac{w_c}{2s}} + j) = -(1 + O(\frac{w_c}{s}))J_0(-j\sqrt{\frac{2s}{w_c}}) \quad (5)$$

In the limit  $s \rightarrow +j\infty$ , the term  $O(w_c/s)$  becomes negligible. Using (5) with  $O(w_c/s)$  omitted, in the limit  $s \rightarrow +j\infty$ ,  $Z_i$  in (4) reduces to

$$Z_i = 0.25R_0 + 0.5R_0\sqrt{\frac{2s}{w_c}} \quad (6)$$

Curves of the real and the imaginary part of  $Z_i/R_0$  versus  $w/w_c$  are shown in comparison with those of  $0.25 + 0.5\sqrt{2s/w_c}$ , a special case of  $A + B\sqrt{s}$ , in Figure 1. It can be seen that (6) is a reliable approximation at higher frequencies. Note also that the skin

impedance always increases the resistance but also adds the inductive impedance. Hence, contradictory to the common belief that skin effect may decrease inductive effects, in many cases the added inductive impedance may outweigh the increase in resistance, resulting in higher inductive effects.

Although at low frequencies, e.g.,  $w < 4w_c$ ,  $Z_i/R_0$  differs significantly from  $0.25 + 0.5\sqrt{2s/w_c}$ , replacing  $Z_i/R_0$  with  $0.25 + 0.5\sqrt{2s/w_c}$  for the entire frequency range does not introduce large errors in the calculated time domain response of *RLC* interconnect circuits. The reason is that *RLC* interconnect circuits are low pass filters, meaning that values of the skin effect impedance at very low frequency do not play important roles in the signal characteristic. For instance, the dc values of the voltage drops on the capacitors in Figure 2 are not affected at all by the inductance and resistance values in the circuit. Therefore only in a portion of the frequency range  $[0, 4w_c]$  will the discrepancy between the exact and the approximated impedance contribute to small errors in the calculated responses. This behavior is illustrated in Figure 5.

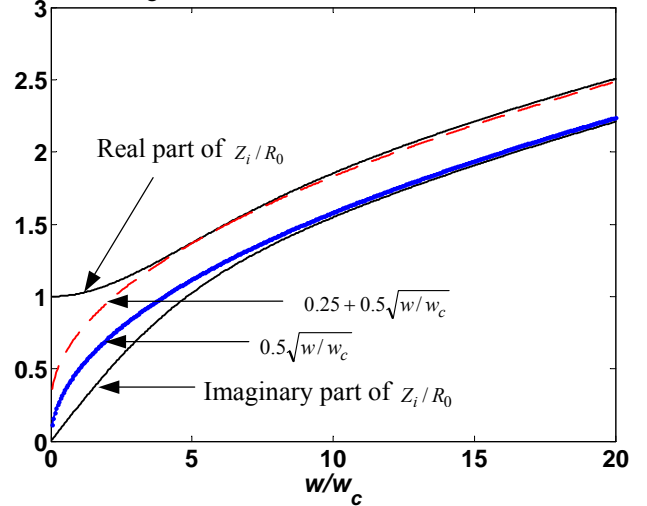


Figure 1. Exact skin effect impedance versus approximate skin effect impedance of round wires

### 3. SQUARE ROOT MOMENTS

One simple structure of *RLC* interconnect circuits is a tree. For a general *RLC* tree (e.g., a tree of 3 *RLC* branches as in Figure 2), the node voltage at node  $i$  is given by

$$V_i(s) = V_{in}(s) - \sum_k C_k V_k(s) s [R_{ki}(s) + L_{ki}s] \quad (7)$$

where  $V_{in}(s)$  represents the input voltage,  $R_{ki}(s)$  represents the total frequency dependent resistance shared by paths from the input port to node  $i$  and from the input port to node  $k$ , and  $L_{ki}$  represents the total inductance shared by paths from the input port to node  $i$  and from the input port to node  $k$ .

The skin effect makes  $R_{ki}(s)$  frequency dependent, which, according to the expression of the skin effect impedance  $A + B\sqrt{s}$  [6-8], consists of two parts, defined as  $R_{dki}$  and  $R_{aki}\sqrt{s}$  for the dc and ac terms of the impedance, respectively. Therefore  $V_i(s)$  can be re-expressed as

$$V_i(s) = V_{in}(s) - \sum_k C_k V_k(s) s [R_{dki} + R_{aki} \sqrt{s} + L_{ki} s] \quad (8)$$

The normalized transfer function  $H_i(s)$  at node  $i$  is the voltage  $V_i(s)$  when a unit impulse ( $V_{in}(s) = 1$ ) is applied to the tree

$$H_i(s) = 1 - \sum_k C_k H_k(s) s [R_{dki} + R_{aki} \sqrt{s} + L_{ki} s] \quad (9)$$

As the  $\sqrt{s}$  term represents singularity at  $s = 0$ ,  $H_i(s)$  cannot be expanded in powers of  $s$ . To overcome this problem, a symbol  $y$  is introduced to replace  $\sqrt{s}$  and  $H_i(s)$  becomes a function of  $y$

$$H_i(y) = H_i(\sqrt{s}) = 1 - \sum_k C_k H_k(y) y^2 [R_{dki} + R_{aki} y + L_{ki} y^2] \quad (10)$$

$$= m_0^i + m_1^i y + m_2^i y^2 + \dots + m_n^i y^n + \dots$$

The relation between  $H_i(y)$  and the square root moment  $m_n^i$  at node  $i$  is

$$m_n^i = \frac{1}{n!} \left. \frac{d^{(n)} H(y)}{dy^n} \right|_{y=0} \quad (11)$$

Using (10) and (11), the moments are obtained as

$$m_0^i = 1 \quad (12)$$

$$m_1^i = 0 \quad (13)$$

$$m_2^i = -\sum_k C_k R_{dki} \quad (14)$$

$$m_3^i = -\sum_k C_k R_{aki} \quad (15)$$

$$m_n^i = -\sum_k C_k (m_{n-2}^k R_{dki} - m_{n-3}^k R_{aki} - m_{n-4}^k L_{ki}), \quad (n \geq 4) \quad (16)$$

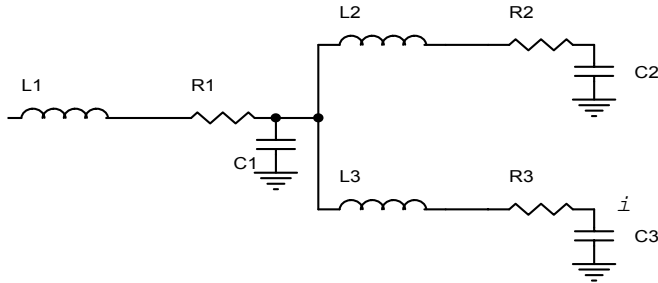


Figure 2. Example of a RLC tree

Note that these moments fall back to the  $s$  moments when  $R_{aki} = 0$  since the odd square root moments become zeros. The closed form solutions above are not valid for circuits with resistive loops, e.g., grids as shown in Figure 3. A set of state variables consisting of the node voltage and the inductor or resistor current will be needed to characterize the circuit. For resistors connected between two capacitors in RLC interconnect circuits of constant elements, there is no need to assign the resistive current as a state variable. However, if the resistance is frequency dependent, the resistive current is assigned as a state variable. In case the inductive current is the same as the resistive current, then only the inductor current is taken as a state variable. Finding node voltages requires solving a set of equations that relate all the node voltages and inductive or resistive currents. For a circuit of  $N$  state variables, the application of Kirchhoff's current law to the node, with that a node voltage defined as a state variable, and the application of Kirchhoff's voltage law to the

elements joining two adjacent nodes lead to the matrix equation given by

$$A_1 X(s) = \sqrt{s} A_2 X(s) + s A_3 X(s) + B_1 U(s) \quad (17)$$

where  $U(s)$  represents  $p$  inputs to the circuit and  $X(s)$ ,  $A_1$ ,  $A_2$ ,  $A_3$ , and  $B_1$  represent  $N \times 1$ ,  $N \times N$ ,  $N \times N$ ,  $N \times N$ , and  $N \times p$  matrices, respectively. Each element of vector  $X(s)$  is either a node voltage or an inductive or resistive current.

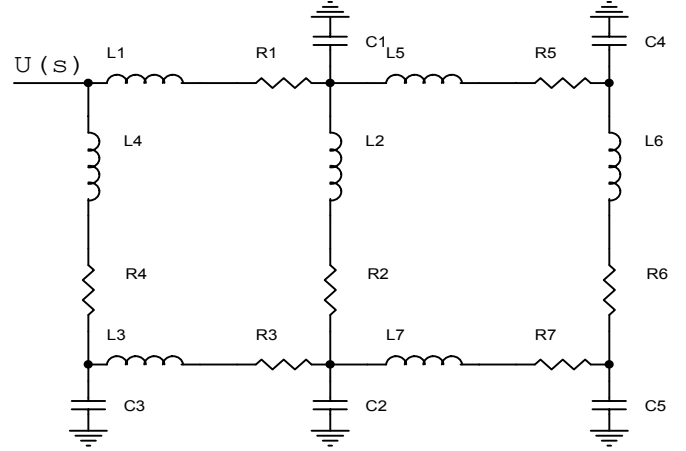


Figure 3. An example of RLC grid

A simple example of forming (17) is given for a single level RLC circuit as shown in Figure 4. A voltage  $U(s)$  is applied to the input port and a current  $I(s)$  is generated to flow through the resistance  $R_d + R_a \sqrt{s}$ , the inductance  $L$ , and the capacitance  $C$  to ground. Denoting the voltage drop on the capacitor as  $V(s)$ , the following two equations are obtained

$$U(s) - V(s) = (R_d + R_a \sqrt{s}) I(s) + s L I(s) \quad (18)$$

$$I(s) = s C V(s) \quad (19)$$

Rewriting the above equations in the form of (17) results in

$$\begin{bmatrix} R_d & 1 \\ 1 & 0 \end{bmatrix} \begin{bmatrix} I(s) \\ V(s) \end{bmatrix} = \sqrt{s} \begin{bmatrix} -R_a & 0 \\ 0 & 0 \end{bmatrix} \begin{bmatrix} I(s) \\ V(s) \end{bmatrix} + s \begin{bmatrix} -L & 0 \\ 0 & C \end{bmatrix} \begin{bmatrix} I(s) \\ V(s) \end{bmatrix} + \begin{bmatrix} 1 \\ 0 \end{bmatrix} U(s) \quad (20)$$

where  $\begin{bmatrix} I(s) \\ V(s) \end{bmatrix}$ ,  $\begin{bmatrix} R_d & 1 \\ 1 & 0 \end{bmatrix}$ ,  $\begin{bmatrix} -R_a & 0 \\ 0 & 0 \end{bmatrix}$ ,  $\begin{bmatrix} -L & 0 \\ 0 & C \end{bmatrix}$ , and  $\begin{bmatrix} 1 \\ 0 \end{bmatrix}$  correspond to  $X(s)$ ,  $A_1$ ,  $A_2$ ,  $A_3$ , and  $B_1$  in (17), respectively.

There is a simple way to check the singularity of the matrix  $A_1$ . Setting  $s$  equal to zero, (17) reduces to

$$A_1 X(0) = B_1 U(0) \quad (21)$$

In this situation, constant inputs represented by  $U(0)$  are applied to the circuit, and only dc components of node voltages and resistive or inductive currents are considered. Since there is no change in the node voltages, all the resistive or inductive currents are zeros. Visualizing that all the single coupling capacitor between two adjacent nodes is taken away, then the RLC circuit under consideration is split into one or more parts, with each part a set of the maximum number of connected elements. Unless an input is applied to one part, the node voltages in that part are undetermined. When an input is applied, obviously the dc

components of the node voltages in that part are the same as that of the input. Therefore, so long as an input is applied to each part of the  $RLC$  circuit, there is a unique solution to (21), which means that the matrix  $A_1$  is invertible.

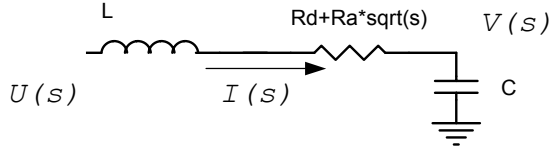


**Figure 4. Single level  $RLC$  circuit**

The output of interest of the  $RLC$  circuit, denote it  $Y(s)$ , is

$$Y(s) = C^T X(s) \quad (22)$$

where  $C^T$  represents a row vector. Assuming matrix  $A_1$  is invertible, the transfer function  $H(s)$  is obtained as

$$H(s) = C^T [I - A_1^{-1} A_2 \sqrt{s} - A_1^{-1} A_3 s]^{-1} A_1^{-1} B_1 \quad (23)$$

Again, as the right hand side of (23) contains  $\sqrt{s}$ , which represents singularity at  $s = 0$ ,  $H(s)$  can't be expanded in powers of  $s$ . This can be overcome by using  $y$  to replace  $\sqrt{s}$  and expanding  $H(y)$  in powers of  $y$

$$[I - A_1^{-1} A_2 y - A_1^{-1} A_3 y^2]^{-1} A_1^{-1} B_1 = M_0 + M_1 y + \dots + M_n y^n + \dots \quad (24)$$

Comparing the coefficients of  $y^n$  on both sides of (24) yields

$$M_0 = A_1^{-1} B_1 \quad (25)$$

$$M_1 = A_1^{-1} A_2 \quad (26)$$

$$M_n = A_1^{-1} A_2 M_{n-1} + A_1^{-1} A_3 M_{n-2}, \text{ for } n \geq 2 \quad (27)$$

These  $M_n$ 's are  $N \times 1$  matrices and fall back to the  $s$  moments if  $A_2 = 0$  since odd moments become zeros. Because there is no requirement on the structure of the  $RLC$  interconnect circuits in deriving the moments  $M_n$ 's, (10) and (12)-(16) for an  $RLC$  tree are just a special case of (24)-(27). In the following sections, only the general equations (24)-(27) are considered.

#### 4. RESPONSES IN TIME DOMAIN

A reduced order transfer function of the form

$$\tilde{H}_n(y) = \frac{1 + a_1 y + a_2 y^2 + \dots + a_{n-1} y^{n-1}}{b_0 + b_1 y + b_2 y^2 + \dots + b_n y^n} \quad (28)$$

is required to approximate the exact transfer function  $H(y)$ . The expansion of  $\tilde{H}_n(y)$  about  $y = 0$  can be selected to match  $2n$  leading coefficients in the expansion of  $H(y)$  since it has  $2n$  variables  $(a_1, \dots, a_{n-1}, b_0, \dots, b_n)$ . By matching the first  $2n$  coefficients in  $H(y)$ , the transfer function  $\tilde{H}_n(y)$  represents a low frequency approximation of  $H(y)$  since higher order terms in the Taylor expansion are negligible at low frequencies. The more the number of coefficients matched, the larger the range of frequency where  $\tilde{H}_n(y)$  is valid.

The coefficient  $b_0$  equals  $1/(C^T M)$  while the coefficients  $b_1, b_2, \dots, b_n$  can be expressed in terms of  $C^T M_0, C^T M_1, \dots, C^T M_{2n-1}$  as [14]

$$\begin{bmatrix} b_n \\ b_{n-1} \\ \vdots \\ b_1 \end{bmatrix} = \frac{-1}{C^T M_0} \begin{bmatrix} C^T M_0 & C^T M_1 & \dots & C^T M_{n-1} \\ C^T M_1 & C^T M_2 & \dots & C^T M_n \\ \vdots & \vdots & \ddots & \vdots \\ C^T M_{n-1} & C^T M_n & \dots & C^T M_{2n-2} \end{bmatrix}^{-1} \begin{bmatrix} C^T M_n \\ C^T M_{n+1} \\ \vdots \\ C^T M_{2n-1} \end{bmatrix} \quad (29)$$

Denoting the zeros and poles of  $\tilde{H}_n(y)$  as  $z_1, \dots, z_{n-1}$  and  $p_1, \dots, p_n$  respectively, (28) can be rewritten as

$$\tilde{H}_n(y) = \frac{1}{y - p_n} \prod_{l=1}^{n-1} \frac{y - z_l}{y - p_l} = \sum_{l=1}^n \frac{k_l}{y - p_l} = C^T M_0 + C^T M_1 y + \dots + C^T M_{2n-1} y^{2n-1} + \dots \quad (30)$$

where  $k_l$ 's satisfy [14]

$$\begin{bmatrix} k_1 \\ k_2 \\ \vdots \\ k_n \end{bmatrix} = - \begin{bmatrix} \frac{1}{p_1} & 0 & \dots & 0 \\ 0 & \frac{1}{p_2} & \dots & 0 \\ \vdots & \vdots & \ddots & \vdots \\ 0 & 0 & \dots & \frac{1}{p_n} \end{bmatrix}^{-1} \times \begin{bmatrix} \frac{1}{p_1} & \frac{1}{p_2} & \dots & \frac{1}{p_n} \\ \frac{1}{p_1^{n-1}} & \frac{1}{p_2^{n-1}} & \dots & \frac{1}{p_n^{n-1}} \end{bmatrix}^{-1} \begin{bmatrix} C^T M_0 \\ C^T M_1 \\ \vdots \\ C^T M_{n-1} \end{bmatrix} \quad (31)$$

If a unit step voltage is applied at the input port, then the output  $Y(y)$  becomes  $\tilde{H}_n(y)/y^2$ . The inverse Laplace transform of  $\tilde{H}_n(y)/y^2$  defines the output in time domain,  $Y(t)$ , that is calculated to be

$$Y(t) = - \sum_{l=1}^n \frac{k_l}{p_l} [1 - (1 - \text{erf}(-p_l \sqrt{t})) e^{p_l^2 t}] \quad (32)$$

where  $\text{erf}()$  stands for the error function. The output can be similarly calculated for arbitrary inputs.

The output  $Y(t)$  is stable only under condition that either  $p_l$  or  $p_l^2$  ( $l \in [1, n]$ ) lie on the left half of the complex plane. Any response of a real  $RLC$  interconnect circuit is stable, but due to model order reduction and round-off errors in finite-precision arithmetic, some of the calculated  $p_l$  or  $p_l^2$  ( $l \in [1, n]$ ) may lie on the right half of the complex plane, making the output  $Y(t)$  unstable. To remedy this instability, those terms in (32) that contain unstable poles  $p_l$  are simply discarded and  $k_l$ 's in the remaining terms are rescaled such that the stable output takes the expected dc value ( $C^T M_0$ ).

#### 5. PADÉ VIA LANCZOS METHOD

In finite-precision arithmetic, moments directly obtained from (25)-(27) are inherently numerically unstable. In practice, this approach can be used only for moderate values of  $n$ , i.e.,  $n \leq 20$ , almost twice what AWE can achieve for constant elements using traditional moments. In some cases, accurate simulation of  $RLC$  interconnect circuits may require higher order of approximation. To handle these cases, the Padé via Lanczos algorithm (PVL) [15] is modified to include skin effect. However, it should be mentioned here that the run time of PVL with skin effect is longer than explicitly matching the square root moments as described before.

Defining a new state space as

$$X'(y) = \begin{bmatrix} X(y) \\ yX(y) \end{bmatrix} \quad (33)$$

Using (17) and (22), by means of simple matrix calculus, the transfer function is obtained as

$$H(y) = [C^T \quad 0_{1 \times N}] [I_{2N \times 2N} - Ay]^{-1} A_1^{-1} B_1 \quad (34)$$

where  $A = \begin{bmatrix} A_1^{-1} A_2 & A_1^{-1} A_3 \\ I_{N \times N} & 0_{N \times N} \end{bmatrix}$ . PVL generates two sequences of

$N \times n$  matrices  $V_n = [v_1 \quad v_2 \quad \dots \quad v_n]$  and  $W_n = [w_1 \quad w_2 \quad \dots \quad w_n]$  by using the following formulae

$$\begin{aligned} AV_n &= V_n T_n + \underbrace{[0 \quad 0 \quad \dots \quad 0]}_{n-1} \hat{v}_{n+1} \\ A^T W_n &= W_n \tilde{T}_n + \underbrace{[0 \quad 0 \quad \dots \quad 0]}_{n-1} \hat{w}_{n+1} \end{aligned} \quad (35)$$

where  $v_n = \frac{\hat{v}_n}{\sqrt{\hat{v}_n^T \hat{v}_n}}$  and  $w_n = \frac{\hat{w}_n}{\sqrt{\hat{w}_n^T \hat{w}_n}}$ .  $T_n$  and  $\tilde{T}_n$  are

tridiagonal matrices represented as

$$T_n = \begin{bmatrix} t_{11} & t_{12} & 0 & \dots & 0 \\ t_{21} & t_{22} & t_{23} & \ddots & \vdots \\ 0 & t_{32} & t_{33} & \ddots & 0 \\ \vdots & \ddots & \ddots & \ddots & t_{n-1,n} \\ 0 & \dots & 0 & t_{n,n-1} & t_{n,n} \end{bmatrix} \quad (36)$$

$$\tilde{T}_n = \begin{bmatrix} \tilde{t}_{11} & \tilde{t}_{12} & 0 & \dots & 0 \\ \tilde{t}_{21} & \tilde{t}_{22} & \tilde{t}_{23} & \ddots & \vdots \\ 0 & \tilde{t}_{32} & \tilde{t}_{33} & \ddots & 0 \\ \vdots & \ddots & \ddots & \ddots & \tilde{t}_{n-1,n} \\ 0 & \dots & 0 & \tilde{t}_{n,n-1} & \tilde{t}_{n,n} \end{bmatrix} \quad (37)$$

The basis vectors  $v_j$  and  $w_k$  are biorthogonal and satisfy

$$w_j^T v_k = 0 \text{ for all } j \neq k \text{ and } j, k = 1, 2, \dots, n \quad (38)$$

The inverse of the  $n$  eigenvalues of the matrix  $T_n$  are the  $n$  poles in (30). Moreover, the  $n-1$  zeros in (30) are the inverse of the  $n-1$  eigenvalues of the matrix obtained from  $T_n$  by deleting the first row and the first column. In this way, PVL implicitly matches the first  $2n$  square root moments of  $\tilde{H}_n(y)$  in (28) with the first  $2n$  square root moments of the original transfer function  $H(y)$  in (23) or (34) without using (25)-(27).

## 6. SIMULATED DATA

Three simulated step responses of a node voltage in the time domain in a three branches tree are shown in Figure 5. The exact result is obtained by numerically solving the inverse Laplace transform describing the step input response. The closed form expression of skin effect impedance [13], which is complicated and exact containing Bessel functions, was used in getting the exact result. According to Figure 5, the approximate result based on constant  $RLC$  model and moment matching techniques underestimates the propagation delay. The other approximate result based on the skin effect impedance  $A + B\sqrt{s}$  and the square root moments matches the exact result very well.

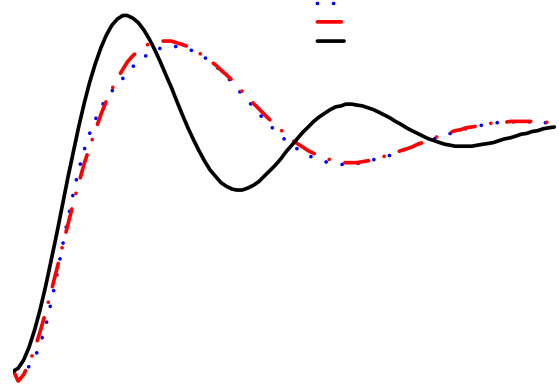


Figure 5. Responses of a  $RLC$  tree

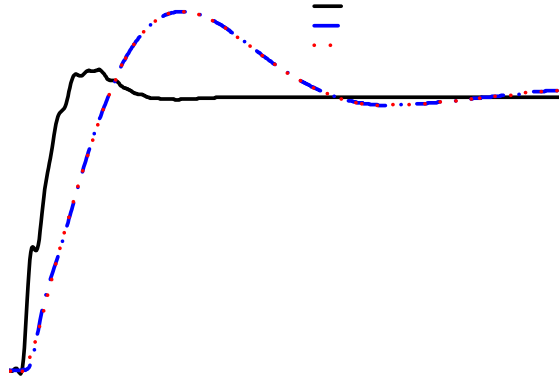


Figure 6. Responses of a  $RLC$  grid

More responses are provided in Figure 6 to Figure 8. Figure 6 shows responses of a large industrial  $RLC$  grid. Figure 7 shows responses of a circuit of a large  $RLC$  tree. Figure 8 shows responses of another industrial circuit that is a combination of an  $RLC$  tree and an  $RLC$  grid. When skin effect is neglected, the PVL (exact) method is used to obtain the responses. When skin effect is considered, both PVL(exact) and square root AWE method are used to obtain the responses, respectively. In each figure, the PVL(exact) and the square root AWE response when skin effect is considered differ significantly from the PVL(exact) response when skin effect is neglected. On the other hand, for responses when skin effect is considered, both square root AWE and PVL(exact) generate very similar curves although PVL(exact) utilizes about 80 moments while square root AWE only utilizes about 30 moments.

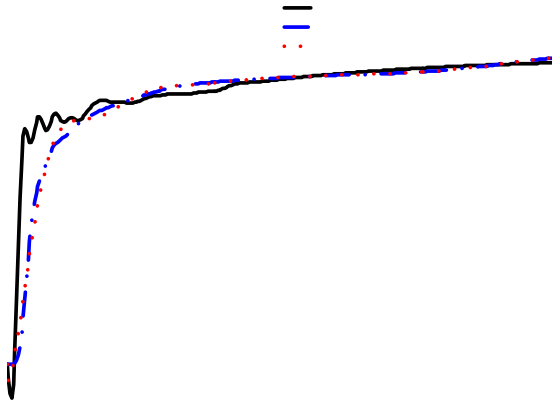


Figure 7. Responses of a RLC tree

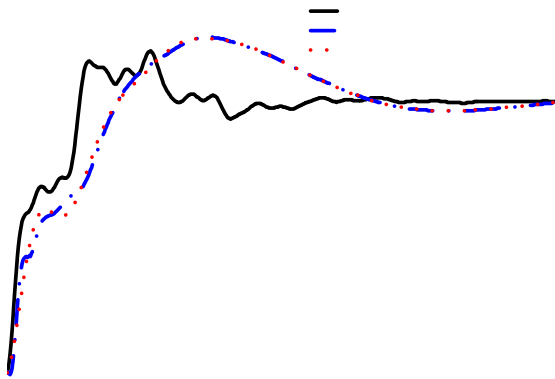


Figure 8. Responses of a combination of RLC tree and RLC grid

## 7. CONCLUSIONS

A new type of moments, namely the square root moments, is defined in this paper to deal with the simulation of RLC interconnect circuits when skin effect is significant. The time to calculate the square root moments is similar to the time to calculate the traditional moments, and the new moments preserve the recursive properties of the traditional moments. In practice, the model order reduction approach based on the square root moments can use almost twice the number of moments that AWE can achieve for constant elements using traditional moments. Also, the PVL method is modified to implicitly match the square root moments. The simulation results reveal the high accuracy of the proposed methods as well as the apparent variation in the signal characteristics caused by skin effect.

## 8. REFERENCES

- [1] D. A. Priore, "Inductance on silicon for sub-micron CMOS VLSI," in *Proc. IEEE symp. VLSI circuits*, May 1993, pp. 17-18.
- [2] "FD-TD modeling of digital signal propagation in 3-D circuits with passive and active loads," *IEEE Trans. Microwave Theory Tech.*, vol. 42, pp. 1514-1523, Aug. 1994. M. P. May, A. Taflove, and J. Baron.
- [3] C.-S. Yen, Z. Fazarinc, and R. L. Wheeler, "Time-domain skin-effect model for transient analysis of lossy transmission lines," *Proceedings of the IEEE*, vol. 70, pp. 750-757, 1982.
- [4] T. V. Dinh, B. Cabon, and J. Chilo, "New skin-effect equivalent circuit," *Electronic Letters*, vol. 26, pp. 1582-1584, 1990.
- [5] A. R. Djordevic, T. K. Sarkar, "Closed-form formulas for frequency dependent resistance and inductance per unit length of microstrip and strip transmission lines," *IEEE Transactions on Microwave Theory and Techniques*, Vol. 42, pp. 241-248.
- [6] N. S. Nahman and D. R. Holt, "Transient analysis of coaxial cables using the skin effect approximation  $A+B\sqrt{s}$ ," *IEEE Transactions on Circuit Theory*, Vol. 19, pp. 443-451, 1972.
- [7] L. C. Calvey and J. L. Bihan, "Coefficient algorithm for time-domain response of skin effect lossy coaxial cables with arbitrary resistive terminations," *IEEE Trans. on Circuit and Systems*, vol. 9, pp. 915-920, Sept. 1986.
- [8] E. Bogatin, M. Resso, S. Corey, "Practical characterization and analysis of lossy transmission lines," *DesignCon 2001*, Santa Clare, CA, Jan. 2001.
- [9] L. T. Pillage, R. A. Rohrer, "Asymptotic waveform evaluation for timing analysis," *IEEE Trans. Computer-Aided Design*, vol. 9, pp. 352-366, Apr. 1990.
- [10] W. C. Elmore, "The transient response of damped linear networks with particular regard to wideband amplifier," *J. Appl. Phys.*, Vol. 19, pp. 55-63, 1948.
- [11] J. L. Wyatt, *Circuit analysis, simulation and design*. North-Holland, The Netherlands: Elsevier Science, 1987.
- [12] Y. I. Ismail, E. G. Friedman, and J. L. Neves, "Equivalent elmore delay for RLC trees," *IEEE Transactions on Computer Aided Design of Integrated Circuits and Systems*, Vol. 19, pp. 83-97, 2000.
- [13] S. Ramo, J. R. Whinnery, and T. V. Duzer, *Fields and waves in communication electronics*, New York: John Wiley & Sons, 1994.
- [14] L. T. Pillage, R. A. Rohrer, and C. Visweswariah, *Electronic circuit and system simulation methods*, McGraw-Hill, 1995.
- [15] P. Feldmann and R.W.Freund, "Efficient linear circuit analysis by Padé approximation via the Lanczos process," *IEEE Trans. Computer-Aided Design*, vol. 14, pp. 639-649, May 1995.